

NOTICE CONCERNING COPYRIGHT RESTRICTIONS

This document may contain copyrighted materials. These materials have been made available for use in research, teaching, and private study, but may not be used for any commercial purpose. Users may not otherwise copy, reproduce, retransmit, distribute, publish, commercially exploit or otherwise transfer any material.

The copyright law of the United States (Title 17, United States Code) governs the making of photocopies or other reproductions of copyrighted material.

Under certain conditions specified in the law, libraries and archives are authorized to furnish a photocopy or other reproduction. One of these specific conditions is that the photocopy or reproduction is not to be "used for any purpose other than private study, scholarship, or research." If a user makes a request for, or later uses, a photocopy or reproduction for purposes in excess of "fair use," that user may be liable for copyright infringement.

This institution reserves the right to refuse to accept a copying order if, in its judgment, fulfillment of the order would involve violation of copyright law.

Impact of Reservoir Permeability on the Choice of Subsurface Geothermal Heat Exchange Fluid: CO₂ Versus Water and Native Brine

Jimmy B. Randolph and Martin O. Saar

Department of Earth Sciences, University of Minnesota, Minneapolis MN

rando035@umn.edu • saar@umn.edu

Keywords

CPG, geothermal, carbon dioxide sequestration, numerical simulation, heat transfer, EGS

ABSTRACT

Geothermal systems utilizing carbon dioxide (CO₂) as the subsurface heat exchange fluid in naturally porous, permeable geologic formations have been shown to provide improved geothermal heat energy extraction, even at low resource temperatures. Such systems, termed CO₂ Plume Geothermal (CPG) systems, have the potential to permit expansion of geothermal energy utilization while supporting rapid implementation through the use of existing technologies. Here, we explore CPG heat extraction as a function of reservoir permeability and in comparison to water and brine geothermal heat extraction. We show that for reservoir permeabilities below 2×10^{-14} to 2×10^{-13} m², depending on formation temperature and pressure, CPG provides better electric power production efficiency than both water- and brine-based systems.

Introduction

Geothermal energy offers clean, reliable, and renewable electric power with no need for grid-scale energy storage. To support future investment in, and growth of, the industry, and to ensure geothermal plays a large role in the future energy landscape, new technology will be critical. Here, we further discuss a new method with the potential to permit widespread expansion of geothermal energy utilization: CO₂ Plume Geothermal (CPG) systems.

Carbon dioxide sequestration in deep saline aquifers and as a component of enhanced oil and hydrocarbon recovery (EOR) has been widely considered as a means for reducing anthropogenic CO₂ emissions to the atmosphere (e.g., 2007 Intergovernmental Panel on Climate Change (IPCC) Fourth Assessment [IPCC, 2007]). However, rather than treating CO₂ as a waste fluid in need of disposal, we propose that it could also be used as a working fluid in geothermal energy capture, as previous studies (e.g., [Randolph and Saar, 2010; 2011b]) suggest it transfers heat more efficiently

than water. Therefore, using CO₂ as a subsurface geothermal working fluid may permit use of lower temperature and lower permeability geologic formations than those currently deemed economically viable. Furthermore, CPG reduces electricity-related CO₂ emissions through both geologic CO₂ sequestration and displacement of hydrocarbon-based power.

CPG systems involve pumping CO₂ into deep, naturally porous and permeable geologic formations where the CO₂ displaces native reservoir fluid and is heated mainly by the natural in-situ heat and by the background geothermal heat flux. A portion of the heated CO₂ is piped to the surface, providing energy for electricity production or direct heat utilization, before being returned to the subsurface. The injected CO₂ is permanently stored via geologic sequestration.

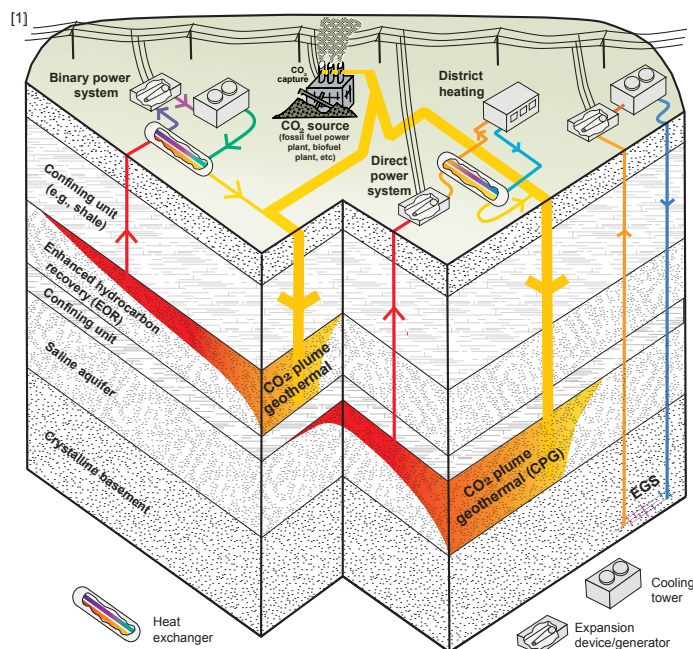


Figure 1. Several envisioned implementations of CO₂-based geothermal systems (reproduced with permission from Randolph and Saar [2011b]).

Traditional water-based geothermal development requires three geologic conditions are met: 1) significant amounts of water as heat capture fluid, 2) a permeable formation to permit water extraction/reinjection, and 3) sufficient subsurface temperatures. Enhanced geothermal systems (EGS) seek to artificially generate Condition 2 and supply (water-based EGS) or avoid (CO₂-based EGS, e.g. [Brown, 2000; Pruess, 2006]) Condition 1, thereby expanding geothermal heat mining prospects. CPG systems, in addition to avoiding Condition 1, reduce minimum thresholds of economically and technologically viable subsurface temperatures (Condition 3), as the high mobility of CO₂ compared to water enhances heat extraction efficiency.

Existing literature [Randolph and Saar, 2010, 2011b] has noted that the high mobility of CO₂ compared to water at the geologic conditions of interest for natural-reservoir-based geothermal development should permit CPG development in reservoirs with permeabilities lower than are viable for water-based geothermal (Condition 2, previous paragraph). Here, we explore geothermal heat extraction from naturally permeable, porous geologic formations as a function of reservoir permeability and subsurface heat exchange fluid.

Numerical Simulation Methodology

The purpose of the investigation detailed here is to isolate the effects of permeability and choice of subsurface heat extraction fluid on natural-reservoir-based geothermal energy production. To accomplish a comparison of reservoir behavior between fluids, numerous assumptions and simplifications to the system are incorporated into the numerical simulations.

First, we assume sufficient geologic formation injectivity/productivity in the immediate neighborhood of wells (bottom hole) for the specified injection/production rates. Though injectivity/productivity are important considerations, the current focus is on reservoir-scale properties. Insufficient well bottom-hole properties could be addressed in part through the use of limited hydraulic, thermal, or chemical stimulation or horizontal wells with long sections open to the reservoir. Similarly, technologies exist to increase the effective well bore diameter.

We simulate operation of geothermal reservoirs containing CO₂, pure water (henceforth called “water”), or 20% mass fraction NaCl brine (henceforth called “brine”) over a variety of reservoir permeabilities, from 5×10^{-16} to 5×10^{-12} m² (see, e.g., Finley [2005] and Steadman et al. [2006] for sample CO₂ sequestration reservoirs with permeabilities covering this range and fluid compositions similar to this brine). In each numerical model, only one fluid occupies the pore space, analogous to previous CPG studies [Randolph and Saar, 2010, 2011b] and CO₂-based EGS studies [Pruess, 2006, 2008]. Thus, in the case of CO₂ working fluid, the presence of subsurface CO₂ is assumed (naturally or from previous injection), and while displacement of native fluid – such as water, brine, or hydrocarbons – is of interest, it is beyond the scope of the present study. All reservoir simulations utilize the simulator TOUGH2 [Pruess, 2004] with equation-of-state module ECO2N [Pruess, 2005].

Of particular interest in the current study are low-temperature geothermal resources, as they provide an opportunity for widespread expansion of the geothermal power base. Therefore, a subsurface system initial temperature of $T = 100$ °C, often

considered the lower limit for geothermal electricity production [e.g., Hulen and Wright, 2001], is chosen. In a region with low to moderate geothermal gradients (30-35 °C/km), $T = 100$ °C corresponds to a reservoir depth of 2.5 km, dependent upon local mean annual surface temperature and fluid/rock thermal conductivity. At such low reservoir temperatures and heat flow rates, it is reasonable to assume approximately hydrostatic fluid pressures [Sanyal et al., 2007]. Table 1 presents a list of formation and model parameters, which are generally consistent with previous publications concerning CPG [Randolph and Saar, 2010, 2011a, 2011b]. With such low formation temperatures, the geothermal power system is taken to be a binary system [Sanyal et al., 2007].

Table 1. Summary of parameters used in base-case models. Base-case parameters correspond, in general, to parameters utilized in previous studies [Randolph and Saar, 2010, 2011a, 2011b]. The base-case simulations were utilized to determine mass-flow rate for each fluid at $k = 5 \times 10^{-14}$ m²; this mass-flow rate was then fixed as permeability was varied. See text for additional details.

| Parameters: Base Case | | | |
|-------------------------------------|--|--|--------------------------------|
| Geologic Formation | | Injection/Production Conditions | |
| Formation map-view area | 1 km ² | Average annual surface temperature | 12 °C |
| Thickness | 305 meters | | |
| Permeability, k | 5×10^{-14} m ² | Surface heat rejection temperature | 22 °C |
| Porosity | 10% | | |
| Rock grain density | 2650 kg/m ³ | Well separation | 707.1 meters |
| Rock specific heat | 1000 J/kg/°C | Well pattern | Five-spot |
| Thermal conductivity | 2.1 W/m/°C | Heat extraction rate | 43.6 MW |
| Formation Initial Conditions | | Formation Boundary Conditions | |
| Fluid in pore spaces | All CO ₂ , H ₂ O, or brine | Top/sides | No fluid or heat flow |
| Temperature | 100 °C | Bottom | Heat conduction, no fluid flow |
| Pressure | 250 bar | | |

Long-term fluid behavior in injection and production wells, once rock surrounding the wells has achieved near-equilibrium with well fluid temperatures, can be approximated as isenthalpic [Pruess, 2006]. Accounting for isenthalpic expansion/compression, i.e. Joule-Thompson cooling/heating, is primarily important in CO₂ simulations (Figure 2). The temperature, T , and pressure, P , profiles for CO₂ in the injection well are calculated by Newtonian iteration starting from T, P values at the surface. Fluid injection surface T is set to 22 °C, which is 10 °C higher than the average annual atmospheric (i.e., power system heat rejection) temperature in St. Paul, MN [NCDC]. This is a conservative assumption for heat rejection efficiency of binary geothermal systems [DiPippo, 2007]. Furthermore for CO₂, injection surface pressure is set to 10 bar above saturation pressure (60.0 bar) at injection wellhead temperature, ensuring single phase conditions in surface equipment (of particular value should the reader wish to compare this binary power system with a direct CO₂ turbine system). Because of the low compressibility/expansivity of water and brine, they are assumed to undergo isothermal well flow [Pruess, 2006].

For simplicity, we assume constant fluid production temperature, a reasonable approximation for the first ten years of power plant operation at the specified reservoir and injection/production

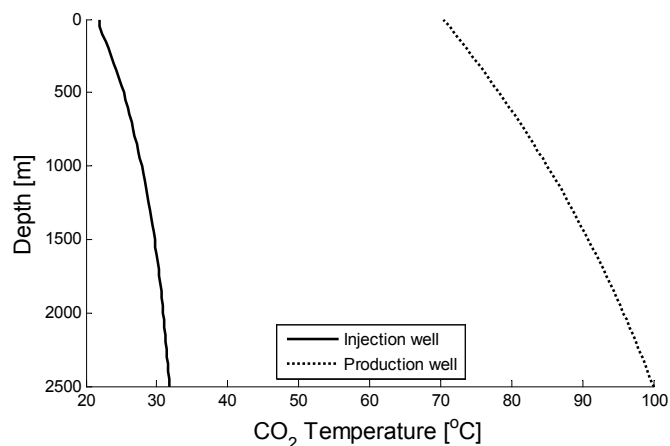


Figure 2. Isenthalpic CO₂ flow in geothermal injection and production wells. Because CO₂ is a relatively compressible supercritical fluid at the temperature and pressure conditions of interest, it compresses/ heats upon injection and expands/ cools during production. Water and brine (not shown), in contrast, are relatively incompressible liquids at the investigated conditions and, thus, experience essentially isothermal well flow.

conditions (see Figure 3 of *Randolph and Saar* [2011b]). Moreover, we ignore the pressure drop through surface equipment (we do, however, impose a mechanical system efficiency of 50%, modified after *Sanyal and Butler* [2005]). While important, this will be explored in future analyses. Note that in certain CPG systems, a throttling valve could be used to sufficiently decrease pressure between injection and production wellheads, whereas in water/brine and other CPG cases (e.g., very low reservoir permeability), additional pumping may be needed.

We account for injection and production pumping power using the approximation given in the U.S. Department of Energy Geothermal Electricity Technology Evaluation Model (GETEM) [Entingh, 2006], where $\text{pumping power} = (\text{total flow}) \times (\Delta P/\rho) \times (\text{pump efficiency})$. Here, ΔP is the required pressure rise to ensure the total flow rate, and ρ is fluid density. Pump efficiency is set conservatively high, to 0.9 (modified from *Sanyal et al.*, [2007]). In CPG simulations, pumping power is assumed to be zero if the production wellhead pressure is higher than the injection wellhead pressure (i.e., a thermosyphon exists). Assuming use of downhole shaft pumps (as opposed to electric submersible pumps, which are not yet in extensive operation), pump depth is limited to 450 m [Sanyal et al., 2007]. Thus, for water and brine models, the assumption of approximately hydrostatic reservoir conditions imposes a minimum pressure of ~ 205 bar at the production well bottom hole such that the fluid will reach the downhole production pump. In simulations, the production bottom hole pressure is not permitted to fall below 210 bar and any additional fluid-driving pressure differential between injection and production wells must come from the injection side.

Reservoir thermal energy extraction rate, H , is calculated from specific enthalpy difference between produced, h , and injected, h_o , fluids, and the production fluid mass rate, Q , given as $H = Q(h - h_o)$. Electricity production rate, E , is then calculated by multiplying H by the Carnot efficiency – calculated using fluid wellhead temperature and the previously-stated mean annual surface temperature (12 °C) – and by a 50% mechanical system efficiency (modified after *Sanyal and Butler* [2005]).

Finally, there are many means that could be employed to compare the CO₂, water, and brine systems. For instance, we could use the same fixed bottom-hole pressure difference between injection and production wells for all fluids, as in previous studies [Pruess, 2006; *Randolph and Saar*, 2010, 2011b]. Alternatively, we could set the production mass flow rate or the binary system power output to be the same for all fluids. However, in order to isolate the effects of reservoir permeability, k , from differences in mobility (inverse kinematic viscosity) and heat capacity of the fluids, we choose to fix the reservoir heat energy extraction rate between fluids for a given reservoir permeability (see *Randolph and Saar* [2011b] for additional information on fluid mobility differences and consequences for reservoir heat extraction). To determine a heat extraction rate to use in comparisons, we start (for consistency with previous literature [*Randolph and Saar*, 2010, 2011b]) with the base case model parameters given in Table 1 (note, $k = 5 \times 10^{-14} \text{ m}^2$). Beginning with the CO₂ case, fluid flow is driven by a 20 bar pressure drop through the reservoir. The CPG heat extraction rate is then determined. For water and brine simulations at the same permeability, the pressure drop through the reservoir is adjusted to match the CO₂ heat extraction rate. The pressure drops specify a mass-flow rate for each fluid, which is fixed as permeability is varied.

Note that these simulations do not necessarily optimize power plant electricity production for each permeability and fluid. For example, a CPG reservoir with high permeability (e.g., $5 \times 10^{-12} \text{ m}^2$) would likely have a power system designed to operate at higher fluid mass-flow rates than that used in this set of simulations. However, in order to compare various reservoir fluids over a variety of permeabilities, fluid mass-flow rates are fixed.

Results: Electricity Production Efficiency Versus Reservoir Permeability

Figure 3 presents geothermal electricity production efficiency versus reservoir permeability for CO₂, water, and brine subsurface working fluids. Electricity production efficiency is defined as the net electricity production rate, E_{net} , divided by the total heat energy extraction rate, H ; E_{net} is the gross electricity production rate, E , minus injection/production pumping power requirements.

For reservoir permeabilities below approximately $2 \times 10^{-14} \text{ m}^2$, CO₂ provides clearly higher electricity production efficiency than both water and brine (see [B] in Figure 3). For larger permeabilities of $k > 2 \times 10^{-14} \text{ m}^2$, pure water, and for $k > 5 \times 10^{-14} \text{ m}^2$ (see [A] in Figure 3), brine is more efficient than CO₂. At moderate to low permeabilities of about $10^{-16} < k < 10^{-14} \text{ m}^2$, CO₂'s high mobility compared to water and brine [*Randolph and Saar*, 2011b] is particularly advantageous as it minimizes pumping power requirements while permitting high mass flow rates. Within this latter permeability range, some k values are so low that net electricity production with pure water, let alone brine, is not possible, while CO₂'s efficiency is hardly diminished (Figure 3). However, at higher permeabilities, the relatively high heat capacity and low compressibility of liquid water and brine, compared to CO₂, result in water and brine having moderately more favorable electricity production efficiencies. At very high permeabilities of about $k > 5 \times 10^{-13} \text{ m}^2$, pumping power (for water and brine) nears zero (while

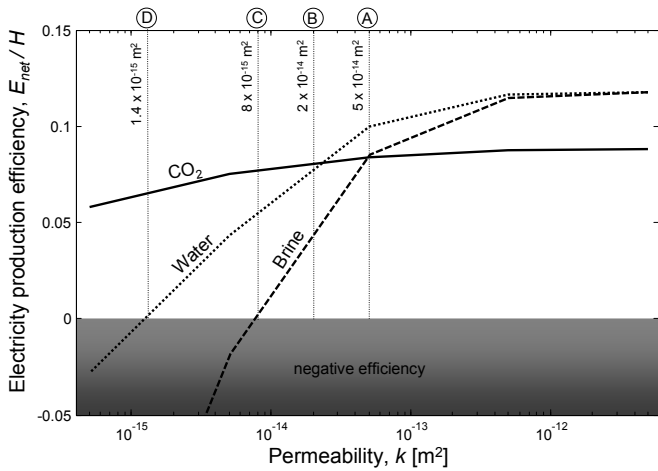


Figure 3. Results of numerical simulations of electricity production efficiency (net electricity production divided by thermal energy extracted from the reservoir) versus reservoir permeability, k , for CO_2 , water, and 20% mass fraction NaCl brine working fluids. For $k < 5 \times 10^{-14} \text{ m}^2$ [A], CO_2 results in higher efficiencies than brine, and for $k < 2 \times 10^{-14} \text{ m}^2$ [B], CO_2 efficiencies are higher than those of water. At $k = 8 \times 10^{-15} \text{ m}^2$ [C], brine transitions into the negative efficiency field while CO_2 results in $\sim 50\%$ higher efficiency than water. At about $k < 1 \times 10^{-15} \text{ m}^2$ [D], water results in negative efficiencies while CO_2 efficiencies remain relatively constant and high. This illustrates that CO_2 is particularly advantageous at somewhat low, but common, permeabilities where water or brine could not be used.

CO_2 does not require pumping due to a strong thermosyphon effect) and electricity production efficiency ceases changing with k .

It should also be noted that aspects other than efficiency, such as undesirable subsurface loss of water versus desirable subsurface loss of CO_2 , i.e. geologic storage, must be considered when selecting a subsurface working fluid. Particularly in arid regions and/or localities where large amounts of CO_2 need to be sequestered, CO_2 may be the preferable subsurface working fluid despite somewhat lower efficiencies than water at higher permeabilities.

The above efficiency results are reasonable in light of the common observation that significant advective heat transfer by water (or brine) appears to require minimum permeabilities of $5 \times 10^{-17} < k_{\min} < 10^{-15} \text{ m}^2$ (e.g., Manning and Ingebritsen [1999], Saar [2011]), given the hydraulic head gradients, water kinematic viscosities, and water heat capacities at temperatures and pressures of interest. Hence, Figure 3 shows how supercritical CO_2 's differing kinematic viscosity (or mobility), heat capacity, and compressibility combine to provide improved geothermal heat extraction – and ultimately electricity production – efficiencies at permeabilities at or below k_{\min} for water. In other words, k_{\min} for CO_2 appears to be several orders of magnitude lower than that for water, and only at permeabilities above k_{\min} is significant advective heat transfer, and resultant economical geothermal energy extraction, expected.

In order to explore the effects of permeability on electricity production efficiency over a variety of temperature and pressure conditions, simulations are executed at several points along two different geothermal gradients, the results of which are given in Figure 4. In Panels [A], [B], and [C] of Figure 4, a geothermal gradient of $35 \text{ }^\circ\text{C}/\text{km}$ (with $12 \text{ }^\circ\text{C}$ as the average annual surface temperature) is utilized, representing a moderate geothermal heat

flow as mentioned above. Note that Panel [B] provides the same results as Figure 3, allowing comparison with other panels. Figure 4 Panels [D], [E], and [F] represent a geothermal gradient of $60 \text{ }^\circ\text{C}/\text{km}$, consistent with a relatively high geothermal heat flow rate, more typical of tectonically and/or volcanologically active regions. Depending on temperature and pressure, Figure 4 shows that CO_2 provides higher electricity production efficiencies than water at permeabilities as high as $2 \times 10^{-13} \text{ m}^2$ (Panel [A]) and than brine at permeabilities of up to $4 \times 10^{-13} \text{ m}^2$ (Panel [A]).

At the other end of the spectrum (Panel [C]), water efficiency remains above that of CO_2 throughout the investigated permeability range, while brine efficiency is greater than that of CO_2 at permeabilities higher than $2 \times 10^{-14} \text{ m}^2$ (panel [C]). Finally, in the high geothermal gradient case (Panels [D] through [F]) efficiencies of the three working fluids are very similar at greater depths and associated temperatures (Panels [E] and [F]). However, at shallower depths and lower temperatures (Panel [D]), to which

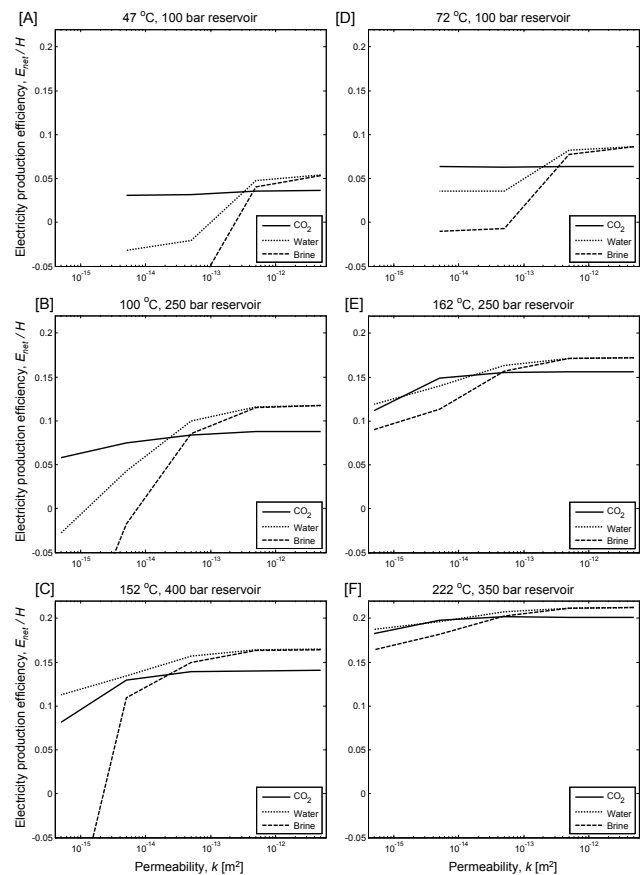


Figure 4. Electricity production efficiency versus permeability, k , for several T, P conditions along two geothermal gradients. In Panels [A], [B], and [C], a moderate geothermal gradient of $35 \text{ }^\circ\text{C}/\text{km}$ (with $12 \text{ }^\circ\text{C}$ average annual surface temperature) is utilized. Note that Panel [B] provides the same results as Figure 3. Panels [D], [E], and [F] represent a relatively high geothermal gradient of $60 \text{ }^\circ\text{C}/\text{km}$. Depending on T, P , CO_2 provides higher electricity production efficiency than water at k as high as $2 \times 10^{-13} \text{ m}^2$ [A]. Similarly, CO_2 provides higher electricity production efficiency than brine at permeabilities as high as $4 \times 10^{-13} \text{ m}^2$ [A]. Note that in the shallow, low temperature cases (Panels [A] and [D]), TOUGH2 simulations did not converge for $k = 5 \times 10^{-16} \text{ m}^2$ because of the very high pressure gradients required to drive flow of cool, dense fluids in such low k reservoirs.

drilling is more economical, CO₂ is more efficient than water at $k < 2 \times 10^{-13} \text{ m}^2$ and than brine at $k < 3 \times 10^{-13} \text{ m}^2$. As previously noted, in all cases, in addition to electricity production efficiency, availability and subsurface loss of water as well as availability and permanent subsurface storage of CO₂ must be considered when selecting a working fluid in real-world applications.

As geothermal development in sedimentary basins progresses, it is likely that at the depths required to achieve sufficient temperatures for economical geothermal development, permeability may be well below $2 \times 10^{-14} \text{ m}^2$ as a result of 1) compaction (of sediments) and/or 2) hydrothermal alteration causing clogging of pore space (e.g., see Finley [2005] and Steadman et al., [2006] for permeabilities, k , of deep sedimentary basins). Moreover, in crystalline rocks, k can be small even at shallower depths. Thus, the results of this investigation are relevant for CPG-type development in sedimentary basins as well as moderately-permeable EGS in crystalline rocks.

Conclusions

Previous studies (Randolph and Saar, 2010, 2011b) have shown that CO₂-plume geothermal (CPG) systems provide higher geothermal heat extraction rates from naturally permeable, porous geologic formations, such as sedimentary basins, than traditional water-based reservoir geothermal operations even at low subsurface temperatures. The work presented here demonstrates that CO₂ is particularly beneficial as a subsurface geothermal heat exchange fluid in moderate-to-low permeability ($k < 2 \times 10^{-14}$ to $2 \times 10^{-13} \text{ m}^2$, depending on reservoir temperature and pressure) formations. Such geologic reservoirs, overlain by low-permeability caprocks, exist worldwide and are under consideration for geologic CO₂ sequestration (e.g., [Finley, 2005; Metz et al., 2005; Steadman et al., 2006]). Furthermore, the present study shows that even at permeabilities higher than $k = 2 \times 10^{-14}$ to $2 \times 10^{-13} \text{ m}^2$, CO₂'s electricity production efficiency is only slightly lower than that of water or brine, depending on temperature and depth, while providing the additional benefits of preserving water and sequestering CO₂.

Future work will explore the geothermal electricity production efficiency of CO₂, water, and brine accounting for optimization of the power cycle. At low resource temperatures ($T < 150 \text{ }^\circ\text{C}$), water- or brine-based geothermal operations are limited to binary power plants, often utilizing a form of Organic Rankine Cycle [GEA, 2010]. However, because of its low critical temperature (31.1 °C at 73.8 bar), CO₂ could be used directly in a turbine (tolerable levels of contaminants, such as water or sulfur, in the CO₂ will also be examined). Potentially, such a direct system would permit significantly higher electricity production efficiencies than those accounted for with the simple assumptions in the current study. For instance, in the base CO₂ case investigated above ($T = 100 \text{ }^\circ\text{C}$, $P = 250 \text{ bar}$, $k = 5 \times 10^{-14} \text{ m}^2$), the net electricity production rate (E_{net}) is calculated to be 3,664 kW, and the production efficiency is 8.4%. In comparison, work, W , produced from a direct system is given by $W = (\text{total mass flow}) \times (\Delta P/\rho)$, where ΔP is the pressure difference between injection and production wells (at wellheads) and ρ is fluid density. Assuming 93% turbine efficiency and 90% system efficiency [Dostal et al., 2004], $E_{net} = 4,170 \text{ kW}$ and the electricity production efficiency is 9.6%. At

higher resource temperatures and pressures, where the wellhead pressure difference may be much larger, the direct system efficiency may be proportionally even larger.

Acknowledgements

Research support was provided by the Initiative for Renewable Energy and the Environment (IREE), a signature program of the Institute on the Environment (IonE) at the University of Minnesota (UMN) and by the U.S. Department of Energy (DOE) Geothermal Technologies Program under Grant Number DE-EE0002764. Any opinions, findings, conclusions, or recommendations in this material are those of the authors and do not necessarily reflect the views of the DOE, IREE, or IonE. M.O.S. also thanks the George and Orpha Gibson and the McKnight Land-Grant Professorship endowments for their generous support of the Hydrogeology and Geofluids Research Group at the UMN. Finally, we thank the anonymous reviewers.

References

- Brown, D. (2000), A hot dry rock geothermal energy concept utilizing supercritical CO₂ instead of water, in *Proceedings of the Twenty-Fifth Workshop on Geothermal Reservoir Engineering*, pp. 233–238, Stanford University, Stanford, CA.
- DiPippo, R. (2007), Ideal thermal efficiency for geothermal binary plants, *Geothermics*, 36, 276–285.
- Dostal, V., M.J. Driscoll, and P. Hejzlar (2004), A supercritical carbon dioxide cycle for next generation nuclear reactors, *Rep. MIT-ANP-TR-100*, Advanced Nuclear Power Technology Program, Massachusetts Institute of Technology, Cambridge, MA.
- Finley, R. (2005), An assessment of geologic carbon sequestration options in the Illinois basin, *Phase 1 Final Report*, Midwest Geological Sequestration Consortium, Illinois State Geological Survey, Champaign, IL.
- Geothermal Energy Association (GEA) (2010), Geothermal power plants – U.S.A., <http://geo-energy.org/plants.aspx>.
- Hulen, J. B., and P. M. Wright (2001), Geothermal energy: Clean, sustainable energy for the benefit of humanity and the environment, Energy & Geoscience Institute, University of Utah, Salt Lake City, UT.
- Intergovernmental Panel on Climate Change (IPCC) (2007), Climate Change 2007: Migration of Climate Change, Contribution of Working Group III to the Fourth Assessment Report of the Intergovernmental Panel on Climate Change, edited by B. Metz et al., Cambridge Univ.Press, Cambridge, U. K.
- Manning CE, Ingebritsen SE (1999) Permeability of the continental crust: implications of geothermal data and metamorphic systems, *Rev. Geophys.* 37:127–150.
- Metz, B., O. Davidson, H. C. de Coninck, M. Loos, and L. A. Meyer (Eds.) (2005), *IPCC Special Report on Carbon Dioxide Capture and Storage*, Cambridge University Press, Cambridge, GB and New York, NY, US.
- U.S.A. Department of Commerce (DOC), National Oceanic and Atmospheric Administration (NOAA), National Environmental Satellite, Data, and Information Service (NESDIS), National Climate Data Center (NCDC), U.S.A. climate normals 1971-2000, <http://cdo.ncdc.noaa.gov/>.
- Pruess, K. (2004), The TOUGH codes — A family of simulation tools for multiphase flow and transport processes in permeable media, *Vadose Zone J.*, 3, 738–746.
- Pruess, K. (2005), ECO2N: A TOUGH2 fluid property module for mixtures of water, NaCl, and CO₂, *Rep. LBNL-57952*, Lawrence Berkeley National Laboratory, Berkeley, CA.

- Pruess, K. (2006), Enhanced geothermal systems (EGS) using CO₂ as working fluid—a novel approach for generating renewable energy with simultaneous sequestration of carbon, *Geothermics*, 35, 351–367.
- Pruess, K. (2008), On production behavior of enhanced geothermal systems with CO₂ as working fluid, *Energ. Convers. Manage.*, 49, 1446–1454.
- Randolph, J. B., and M. O. Saar (2010), Coupling geothermal energy capture with carbon dioxide sequestration in naturally permeable, porous geologic formations: A comparison with enhanced geothermal systems, *GRC Transactions*, 34, 433–438.
- Randolph, J. B., and M. O. Saar (2011a), Coupling carbon dioxide sequestration with geothermal energy capture in naturally permeable, porous geologic formations: Implications for CO₂ sequestration, *Energy Procedia*, 4, 2206–2213, DOI: 10.1016/j.egypro.2011.02.108.
- Randolph, J. B., and M. O. Saar (2011b), Combining geothermal energy capture with geologic carbon dioxide sequestration, *Geophysical Research Letters*, In Press.
- Saar, M.O. (2011), Review: Geothermal heat as a tracer of large-scale groundwater flow and as a means to determine permeability fields, special theme issue on Environmental Tracers and Groundwater Flow, editor-invited peer-reviewed contribution, *Hydrogeology Journal*, 19:31–52, DOI 10.1007/s10040-010-0657-2.
- Sanyal, S. K., and S. J. Butler (2005), An analysis of power generation prospects from Enhanced Geothermal Systems, in *Proceedings of the World Geothermal Congress*, paper 1632, Antalya, TR.
- Sanyal, S. K., J. W. Morrow, and S. J. Butler (2007), Net power capacity of geothermal wells versus reservoir temperature – a practical perspective, in *Proceeding of the Thirty-Second Workshop on Geothermal Reservoir Engineering*, Stanford University, Stanford, CA.
- Steadman, E. N., D. J. Daly, L. L. de Silva, J. A. Harju, M. D. Jensen, E. M. O’Leary, W. D. Peck, S. A. Smith, and J. A. Sorensen (2006), Plains CO₂ reduction (PCOR) partnership (phase 1) final report/July–September 2005 quarterly report, Energy & Environmental Research Center, University of North Dakota, Grand Forks, ND.